



Heriot-Watt University
Research Gateway

Temperature effects upon a multicore optical fibre curvature sensor

Citation for published version:

Papachristou, N, Morton, J, Carter, RM, Maier, RRJ & Macpherson, WN 2017, Temperature effects upon a multicore optical fibre curvature sensor. in *2017 IEEE SENSORS.*, 8234257, IEEE.
<https://doi.org/10.1109/ICSENS.2017.8234257>

Digital Object Identifier (DOI):

[10.1109/ICSENS.2017.8234257](https://doi.org/10.1109/ICSENS.2017.8234257)

Link:

[Link to publication record in Heriot-Watt Research Portal](#)

Document Version:

Peer reviewed version

Published In:

2017 IEEE SENSORS

Publisher Rights Statement:

© 2017 IEEE. Personal use of this material is permitted. Permission from IEEE must be obtained for all other uses, in any current or future media, including reprinting/republishing this material for advertising or promotional purposes, creating new collective works, for resale or redistribution to servers or lists, or reuse of any copyrighted component of this work in other works.

General rights

Copyright for the publications made accessible via Heriot-Watt Research Portal is retained by the author(s) and / or other copyright owners and it is a condition of accessing these publications that users recognise and abide by the legal requirements associated with these rights.

Take down policy

Heriot-Watt University has made every reasonable effort to ensure that the content in Heriot-Watt Research Portal complies with UK legislation. If you believe that the public display of this file breaches copyright please contact open.access@hw.ac.uk providing details, and we will remove access to the work immediately and investigate your claim.

Temperature effects upon a multicore optical fibre curvature sensor

Nikolitsa Papachristou, Jonathan Morton, Richard M. Carter, Robert R. J. Maier, William N. MacPherson
Institute of Photonics and Quantum Sciences
Heriot-Watt University, Edinburgh, UK

Abstract—We investigate the effect of temperature on a multicore fibre (MCF) curvature sensor. The curvature sensing element is formed from four Fibre Bragg gratings (FBGs) inscribed in a MCF. A fibre optic coupled fan-out device is used to interface the MCF to standard single core fibre optic technology. The peak positions of the FBGs are measured to determine wavelength shift as a result of the curvature induced strain on the fibre. The differential strain allows the curvature of the fibre in a plane to be extracted. The temperature sensitivities of the FBGs and the fan-out device are examined thoroughly.

Keywords— *multicore fibre, strain sensor, fibre Bragg gratings, fan-out device, low coherence interferometry.*

I. INTRODUCTION

Sensing with optical fibres has seen increased application due to the significant advantages that fibre sensors offer over conventional technology [1]. These advantages can include higher resolution and quicker response compared to other techniques. Additionally, the small volume of the optical fibres makes them ideal for applications in confined or remote areas. Fibre sensors can often be embedded into a host structure, this can help protect them and influences their resolution and sensitivity [2]. Practical deployment relies upon the ability to isolate or compensate the sensor from unwanted environmental effects. In this work, we explore the influence of temperature variations on a multicore fibre (MCF) curvature sensor.

II. INSCRIPTION OF MULTICORE FIBRE BRAGG GRATINGS

The four-core MCF curvature sensor was fabricated by inscribing FBGs into all four cores. The magnitude and direction of curvature of the fibre can be determined by monitoring the wavelength shift of the FBGs. The MCF is designed to be single-mode at communication wavelengths with cladding and core diameters of 125 μm and 8 μm respectively. The core separation is 50 μm , effectively eliminating crosstalk between cores. Figure 1 shows a cross section of the MCF fibre.

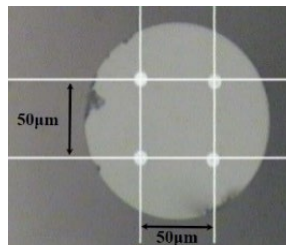


Figure 1. Cross section of the multicore fibre, with cores illuminated with white light for illustration purposes.

FBGs were inscribed into the four cores of the MCF using the phase mask technique to generate the required interference pattern [3]. A Copper vapour laser emitting at 510.6 nm was frequency doubled to 255.3 nm using a BBO (Barium – Borate) crystal. FBGs were produced simultaneously on all four cores of the MCF at the same position along the fibre.

The inscription process was monitored during UV exposure using a commercial optical interrogator. Spectra from each individual core of the MCF were collected using a fan-out device. This device couples light from each core of the MCF into a separate single mode fibre (SMF) and had been fabricated using ultrafast-laser waveguide inscription on a silica glass slide [4]. The MCF section where the FBGs were to be inscribed was spliced in advance on to the fan-out device using a Fujikura FSM-100 P+ splicer. The final arrangement is shown in Figure 2.

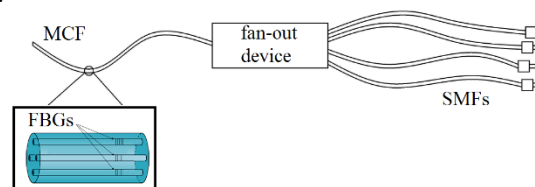


Figure 2. Spliced piece of MCF with Bragg gratings on the fan-out device.

III. TEMPERATURE SENSITIVITY OF THE SENSOR

Orthogonal pairs of cores provide differential strain measurements for two orthogonal directions. This allows the 3D curvature to be monitored [5].

It is expected that all four cores of the MCF are equally affected by temperature changes, since they are positioned close to each other and they are surrounded by the same material. As a result, by monitoring the differential strain between two cores, common mode temperature effects should be eliminated. However, thermal variation of other component properties may affect the measured spectrum, and hence the recovered differential strain.

A. Circular motion of the MCF curvature sensor

The effect of temperature variation on the sensor was tested by monitoring the end position of the MCF while it was moving in a circle of 3 mm radius over a range of temperatures.

The calibration of the sensor was performed with the fan-out device maintained at a stable temperature of 25.5 °C. Figure 3a (black) shows the motion of the tip of the sensor upon circular deflection at 25.5 °C. The same circular deflection was applied while the fan-out device was maintained at temperatures of 24.5 °C and 26.5 °C. Figure 3b shows that the measured motion using the 25.5 °C calibration values for different temperatures of the fan-out device, deviates from the expected circular motion. Finally, by restoring the fan-out device's temperature to 25.5 °C, the circular motion was retrieved (figure 3a - red).

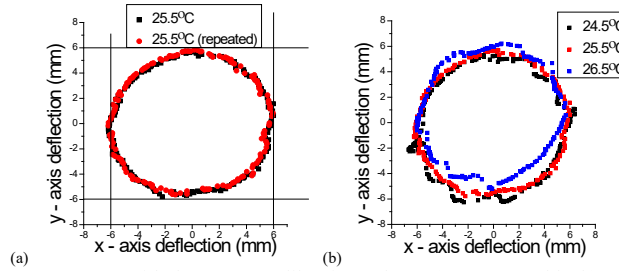


Figure 3. Measured circular motion of the MCF sensor, with the 25.5°C calibration values (a) at 25.5°C (black), repeated at 25.5°C (red) and (b) at different temperatures of the fan-out device.

B. Temperature sensitivity of the FBGs and the fan-out device

Experiments were carried out to determine whether the temperature variations observed were due to the fan-out device, or the FBGs. The fan-out device temperature was stabilized and the MCF with FBGs was placed on a hot plate. Both temperatures were monitored with thermocouples, positioned close to the device and FBGs respectively. No strain was applied to the MCF. Spectra were collected for two cases:

- i. The fan-out was held at, 27 ± 0.2 °C and the hot plate temperature varied from 25 °C to 29 °C. As expected each individual FBG follows the temperature variations (Figure 4a). However, the wavelength shift between two cores is not affected with these variations. There is a small variation at the first 3000 seconds, which is the period where the fan-out device warms up to reach the 27 °C and temperature gradients may exist in the setup (Figure 4b).
- ii. The fan-out device was set in the temperature range of 27.2 – 28.9 °C by increasing it 0.5 °C every 5000 seconds and the FBGs were held at a stable temperature of 29.4 ± 0.2 °C. In this case, the separation between wavelength peaks should be temperature invariant of the fan-out (Figures 5a, 5b). Experiments indicate that there is a wavelength shift of core pairs 1-3 and 1-4 which follow a similar response to the fan-out temperature.

This is an initial indication that coupling of light from the MCF to the SMFs in the fan-out device is affected by temperature. However, the sensitivity of the MCF sensor is only significantly affected when the fan-out's device temperature varies more than 0.3 °C.

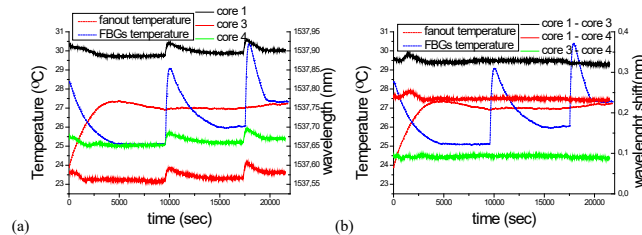


Figure 4. FBG response with fan-out temperature stabilized, and the FBG temperature varied. (a) FBG wavelength, (b) Wavelength shift between core pairs.

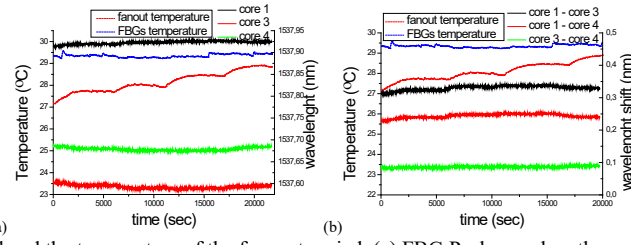


Figure 5. FBGs temperature stabilized and the temperature of the fan-out varied. (a) FBG Peak wavelengths and (b) wavelength shift of core pairs.

C. Temperature sensitivity of the fan-out device

The background of the FBG's spectra can affect the measurement of their peak position, therefore a stable background is required to monitor the exact position of these peaks with high accuracy. The background noise of the MCF was monitored using a section of fibre with no FBGs. This spectrum (Figure 6) was found to have three superimposed sinusoidal patterns, which correspond to one or more interference effects.

To determine the source of these sinusoidal effects, regions of high attenuation of the light was induced by bending the fibre at three different locations. Initially, the bend was applied to the SMF, to test the interface between the interrogator and the connector. In this case the fluctuations were eliminated. The fan-out device was tested by bending the MCF after the device but before the splice point. Two of the sinusoidal patterns remained (Figure 6a and 6c) while one was partially eliminated (Figure 6b). Finally, the splice point was tested by bending the end of the fibre. For this case, the background fluctuations were similar to the previous one. Since the second sinusoidal pattern showed differences by bending the MCF, it can be attributed to interference between higher transmission modes. However, the first and the third patterns remained in all cases when light was coupled through the fan-out device, thus one or more Fabry-Perot optical cavities were believed to be formed in the device. All cores of the MCF show comparable interference patterns and the same behavior at the bending points. Table I shows the optical length of these Fabry-Perot cavities calculated from the observed spectra.

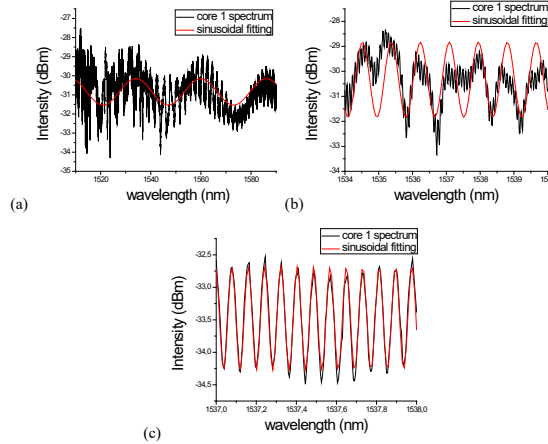


Figure 6. First (a), second (b) and third (c) interference patterns on core 1 spectrum and a sinusoidal fit to recover the effective interference cavity length.

	Optical length (mm)		Optical distance (mm)
	cavity 1	cavity 2	
core 1	0.0438	14.455	14.604
core 2	0.0494	14.452	14.547
core 3	0.0475	14.441	14.546
core 4	0.0429	14.487	14.549
Average	0.0459	14.459	14.561

TABLE I. Fabry-Perot optical cavity lengths determined from the sinusoidal fitting on the spectra collected with the interrogator and optical distances between the two reflections determined from the low coherence interferometry experiment for all MCF cores.

The temperature sensitivity of the background introduced by the fan-out device was studied. Initially, the fan-out remained at a constant temperature (27.8 °C) and as shown in Figure 7a the background noise, shown here for core 1, was stable. These spectra were monitored every 5 minutes for half an hour. However, for different temperatures of the fan-out device (27.5 – 28.8 °C, with 0.4°C step), the background varied (Figure 7b). The same response was observed on all cores of the MCF.

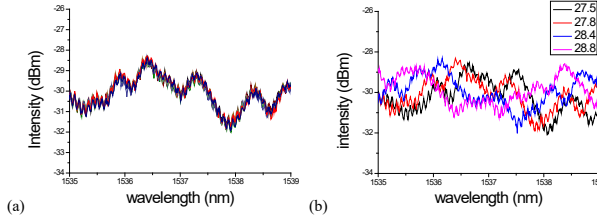


Figure 7. Spectra from the MCF without the FBGs for core 1, (a) fan-out device on stable temperature, (b) fan-out device on different temperatures.

D. Low coherence interferometry

A low coherence interferometry experiment was performed and two different reflections were detected inside the fan-out device [6]. An IR broadband source with central wavelength at 1550 nm was used for this experiment. Figure 8 shows the interference patterns of this experiment, detected in core 1 at two different positions inside the fan-out device. This experiment was repeated several times for all four cores of the MCF, and all show two reflections at the same positions (see table I). The width of the reflection signals introduces an uncertainty on their exact position, thus an error ± 0.1 mm on the distance is considered.

The optical length of the reflections agrees with one of the Fabry–Perot cavity lengths that was identified in the measured reflection spectrum. The measured optical distance between the reflections deviates by only 0.7% from the second cavity length calculated with the Fabry–Perot equation.

Finally, the coherence length of the IR source, measured from its spectrum, is 0.026 mm. This is comparable to the first cavity length calculated from the Fabry–Perot equation. This means that the first cavity length is close to the resolution limit of the low coherence interferometry experiment, thus it was not detectable.

It is believed that the first cavity could be formed at the interface between the inscribed waveguides in the silica glass of the fan-out device and the SMF or MCF fibre. Whereas, the second cavity can be attributed to the beginning and end of the waveguides in the silica glass of the device since the cavity length is comparable to the actual length of the device.

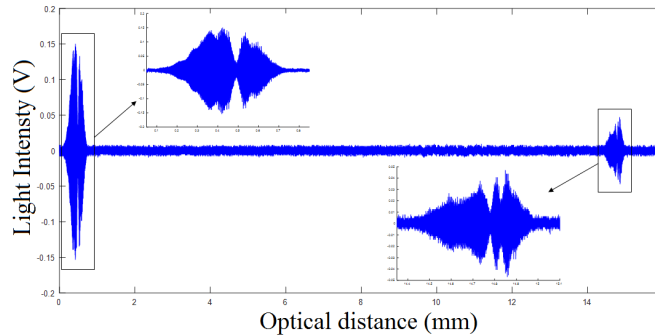


Figure 8. Interference patterns of the two reflections in the fan-out device.

IV. CONCLUSIONS

We studied the temperature sensitivity of a MCF curvature sensor, fabricated by inscribing FBGs into the cores of the fibre with the phase mask technique. The temperature effect on the FBGs is eliminated when the differential wavelength shift of the FBGs between the cores is monitored. However, the coupling of light from the MCF to each individual SMF, in the fan-out device, is affected by temperature. Spectra from the fan-out device showed interference patterns which can be attributed to the formation of Fabry–Perot cavities in the fan-out device. As a result, errors in the calculation of the end position or curvature of the MCF can be introduced. These errors can be eliminated by fabricating the fan-out device with higher precision. Angle cleave on the fibres and on the silica glass edges can be introduced to avoid the creation of the cavities.

ACKNOWLEDGMENTS

The authors would like to acknowledge funding from the European Union’s Horizon 2020 research and innovation programme under grant agreement No 635568: LAKHsMI Project.

REFERENCES

- [1] B. Lee, "Review of the present status of optical fiber sensors," *Optical Fiber Technology*, vol. 9, p. 23, July 2003.
- [2] I. Garcia, J. Zubia, G. Durana, G. Aldabaldetrekua, M. A. Illarramendi, and J. Villatoro, "Optical Fiber Sensors for Aircraft Structural Health Monitoring," *Sensors (Basel)*, vol. 15, pp. 15494-519, 2015.
- [3] K. O. Hill and G. Meltz, "Fiber Bragg Grating Technology Fundamentals and Overview," *Journal of Lightwave Technology*, vol. 15, p. 14, September 1997.
- [4] R. R. Thomson, H. T. Bookey, N. D. Psaila, A. Fender, S. Campbell, W. N. MacPherson, et al., "Ultrafast-laser inscription of a three dimensional fan-out device for multicore fiber coupling applications," *Optics Express*, vol. 15, p. 11691, 2007.
- [5] G. M. H. Flockhart, W. N. MacPherson, J. S. Barton, J. D. C. Jones, L. Zhang, and I. Bennion, "Two-axis bend measurement with Bragg gratings in multicore optical fiber," *Optics Letters*, vol. 28, p. 387, 2003.
- [6] S. Kim, J. Na, M. J. Kim, and B. H. Lee, "Simultaneous measurement of refractive index and thickness by combining low-coherence interferometry and confocal optics," *Optics Express*, vol. 16, pp. 5516-5526, April 2008.